

Electrochemical Impedance Spectroscopy Study of Lime Soil and Interpretation of the Results

Zhiwei Chen, Pengju Han*, Bin He**, Funan Sun, Xiangling Bai, Xinyu Liu, Yuting Wang

College of Civil Engineering, Taiyuan University of Technology, Taiyuan, 030024, China

*E-mail: 13834569544@163.com

**E-mail: hebin@tyut.edu.com

Received: 6 April 2021 / Accepted: 29 May 2021 / Published: 30 June 2021

In this study, data measured by the electrochemical impedance spectroscopy (EIS) method were used to assess the shear strength and unconfined compressive strength of lime soil. Two equivalent circuit models, $R_s(Q(RctW))$ and $R_s(QRct)$, were proposed to explain the EIS results in terms of the physical properties and chemical reactions in lime soil. The experimental results suggest that the peak phase angle value in the Bode plots has a linear relationship with the internal friction angle. The equivalent circuit element parameter Rct is positively correlated with cohesion and unconfined compressive strength, while Q is negatively correlated with these variables. The relationships between cohesion and $\ln(Rct/Q)$ and between unconfined compressive strength and $\ln(Rct/Q)$ all show good linear correlations. Hence, the peak phase angle and equivalent circuit element parameters (Rct , Q) can be applied to assess and predict the shear strength and unconfined compressive strength of lime soil.

Keywords: Electrochemical impedance spectroscopy (EIS); Shear strength; Unconfined compressive Strength; Lime soil

1. INTRODUCTION

Lime soil or lime-treated soil refers to the addition of lime to the soil and has been widely used for centuries in the field of civil engineering, including highways, foundation bases, and pile foundations, among others[1]. So-called 3:7 lime soil (the volume ratio of lime and soil is 3:7) is the most used example. It has been proven that the mixture of lime with soil can improve its mechanical properties, including shear strength and unconfined compressive strength [2, 3]. There are four classic reactions in lime soil[4]: (1) ion exchange; (2) flocculation and agglomeration; (3) pozzolanic reactions; and (4) carbonation. Many researchers attribute the increase in the strength of lime soil to the cementation products (calcium silicate hydrates and calcium aluminate hydrates) formed by the pozzolanic reactions between soil minerals and $(Ca(OH)_2)$ [5-7]. The triaxial compressive test and unconfined compressive

strength test are commonly used to study the mechanical properties of lime soil[8]. However, these tests are complex and destructive methods.

Electrochemical impedance spectroscopy (EIS), which associates dielectric properties with microstructures, is a non-destructive, low-cost, sensitive, and convenient method[9]. In the EIS measurement process, an equivalent circuit model is usually used to model the electrochemical process that occurs in the material, and the equivalent circuit parameters have specific physical meanings. EIS has been applied to investigate pozzolanic reactions and estimate the strength of cement and concrete[10-13]. Like cement and other cementitious materials, lime soil can be regarded as an electrochemical system. Its chemical reactions are complex electrochemical processes involving ion exchange and pozzolanic reactions. Therefore, EIS can be used to investigate the reactions and estimate the strength of lime soil. However, in previous studies, the strength of lime soil was measured through triaxial compressive tests and unconfined compression tests, which are destructive and inconvenient. The application of electrochemical impedance spectroscopy to lime soil and the relationship between the electrical impedance and soil strength have not been studied.

In this study, the EIS test, triaxial compressive test and unconfined compression test were used to evaluate 3:7 lime soil with curing times of 1 d, 2 d, 3 d, 7 d, 14 d, 21 d and 28 d, respectively. Two types of equivalent circuit models that consider the physical behaviour and chemical reactions in lime soil were proposed to analyse EIS data, which allows us to gain a better understanding of the electrical impedance changes of lime soil. This study intends to determine the relationships between EIS results and shear strength and between EIS results and unconfined compression strength. These relationships provide a convenient, fast, simple and feasible way to study the shear strength and unconfined compressive strength of lime soil.

2. MATERIALS AND METHODS

2.1. Materials preparation

2.1.1. Soil

The soil used in this study was collected from a construction site in the eastern part of the city of Taiyuan, Shanxi Province, China. The physical properties and chemical compositions of the soil were obtained by laboratory tests (see Table 1 and Table 2). According to the plasticity index (I_P) and the Chinese standard Code for Investigation of Geotechnical Engineering (GB 50021-2001), this soil was classified as silty clay. In this study, the soil was first air-dried at room temperature and sieved to 5 mm. Then, the soil was dried at 105°C for at least 6 hours until the quality of the soil no longer changed.

Table 1. Physical properties of the soil used in this study.

Density (d_s)	Liquid Limit (w_L)	Plastic Limit (w_P)	Plasticity Index (I_P)
2.71 g/cm ³	32.1%	18.5%	13.6

Table 2. Chemical compositions of the soil used in this study.

SiO ₂	Al ₂ O ₃	Fe ₂ O ₃	CaO	MgO	Others
56.64%	20.32%	8.47%	6.51%	2.15%	5.91%

2.1.2. Lime

This study employed hydrated lime (the content of Ca(OH)₂ was greater than 90%). The hydrated lime was sieved (5 mm), and its density was 2.24 g/cm³.

2.1.3. Water

To prevent adverse reactions and reduce the influence of other ions present in water, distilled water was used to mould and cure the lime soil samples in this study[14].

2.1.4. Lime soil

To obtain the optimal moisture content and maximum dry density of the lime soil by the compaction test, lime soil samples with different water contents were prepared as follows. First, the soil was mixed with distilled water to prepare soil samples with different water contents, and the soil samples were sealed for 24 hours so that the water could evenly distribute through the soil. Then, the hydrated lime was evenly mixed with the soil samples in a 3:7 volume ratio to prepare the 3:7 lime soil samples (referred to as lime soil hereafter). Finally, the compaction test was performed in accordance with the Chinese standard Geotechnical Testing Method (GB/T 50123-2019), and the optimal moisture content and maximum dry density were 24% and 1.474 g/cm³, respectively.

For triaxial compressive and unconfined compression tests, lime soil samples 39.1 mm in diameter and 80 mm in height were moulded. The dry density of the lime soil samples was 98% of the maximum dry density at the optimal moisture content[15]. To prevent significant changes in water content, the lime soil samples were cured in a sealed box for 1 d, 2 d, 3 d, 7 d, 14 d, 21 d and 28 d at 25 ± 2 °C.

2.2. Testing methods

2.2.1. EIS measurements

Because the temperature can have a significant impact on the accuracy of EIS measurements[16], the measurements were carried out at room temperature (25 ± 2)°C by using an electrochemical workstation (CS350H, Wuhan Corrtest Instruments Corp., Ltd, China) with a three-electrode system. During the test, the lime soil sample was placed on a metal base with a plastic support between the sample and base. Two copper sheets were used as electrodes and placed in parallel on the top and bottom

surfaces of the cylindrical lime soil sample and fixed with a clamp so that the electrodes and the lime soil sample were in close contact. Two quartz coverslips were placed between the clamp and the copper sheets. For the three-electrode system, one copper sheet served as the working electrode (WE), and the other served as the counter electrode (CE) and reference electrode (RE). A schematic diagram of the EIS measurement system is shown in Figure 1. When the open circuit potential was stable, an EIS spectrum was measured over the frequency range from 10^5 to 10^{-1} Hz with a sinusoidal voltage signal of 10 mV. To ensure the accuracy and reproducibility of the EIS spectra, each lime soil sample was measured three times.

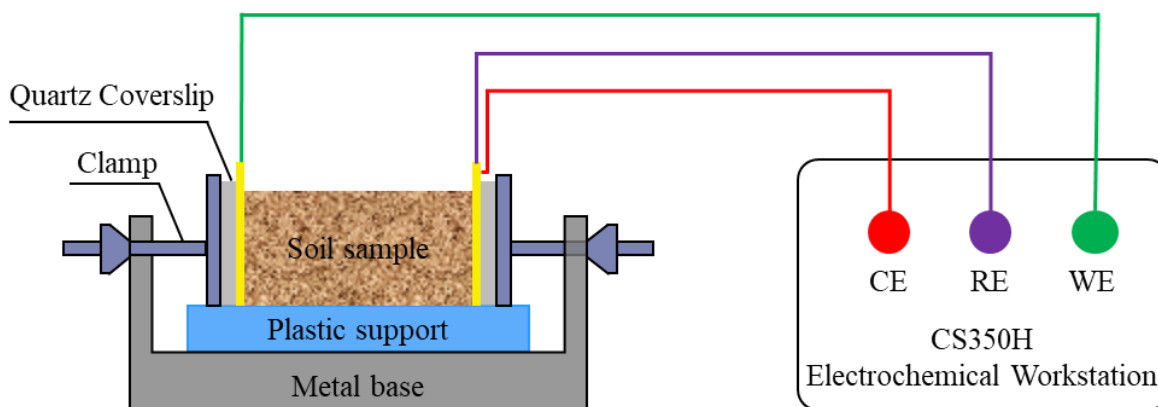


Figure 1. Schematic diagram of the EIS measurements.

2.2.2. Triaxial compressive tests

To obtain the shear strength parameters (cohesion, c ; internal friction angle, φ) of the lime soil samples, the triaxial compressive test was carried out according to the Chinese standard Geotechnical Testing Method (GB/T 50123-2019). Considering that the lime soil used for foundation or construction is usually at its optimum water content, it is impossible to drain water during compression[16]. Therefore, the triaxial compressive test adopted an unconsolidated-undrained (UU) method at a certain confining pressure ($\sigma_3 = 200$ kPa) using a Sigma-1TM Automated Load Test System manufactured by GEOTAC (Geotechnical Test Acquisition & Control, Houston, TX, USA).

At least three lime soil samples were tested for each curing time, and results with an error greater than 10% were discarded. The shear strength parameters at each curing time were reported as the mean value of at least three samples.

2.2.3. Unconfined compression test

The unconfined compression tests were in accordance with the Chinese standard Geotechnical Testing Method (GB/T 50123-2019). The unconfined compression tests were performed with a YSH-2 Lime soil Unconfining Pressure Test Apparatus with a sensitivity of 0.01 mm (Nanjing Soil Instrument

Factory CO., LTD, Nanjing, China). Its maximum capacity is 5 kilonewton (kN), and the speed is 1 mm/min.

Unconfined compressive strength represents the ultimate loading bearing capacity of lime soil. The maximum axial stress on the axial stress-strain curve is taken as the unconfined compressive strength. However, when the maximum axial stress is not available on the axial stress-strain curve, the stress corresponding to the axial strain of 15% is taken as the unconfined compressive strength[8].

At least three lime soil samples were tested for each curing time, and results with an error greater than 10% were discarded. The unconfined compression strength for each curing time was given as the mean of at least three samples.

3. RESULTS AND ANALYSIS

3.1. The reaction mechanism of lime soil

3.2. EIS results

3.2.1. Nyquist plots and equivalent circuit models

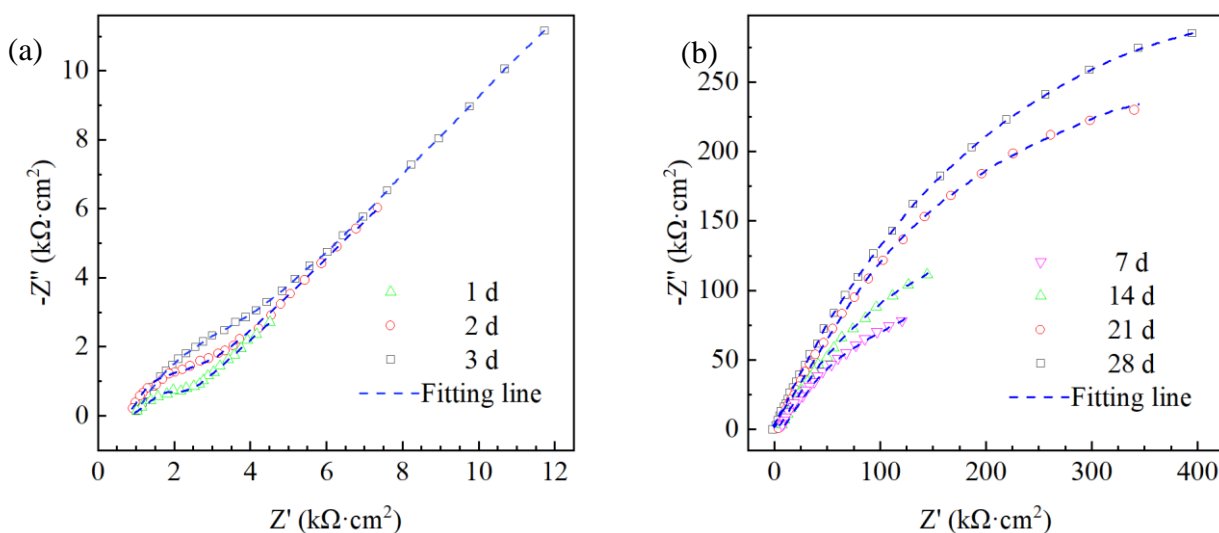


Figure 2. Nyquist plots of lime soil at different curing times: (a) 1 d, 2 d and 3 d, (b) 7 d, 14 d, 21 d and 28 d.

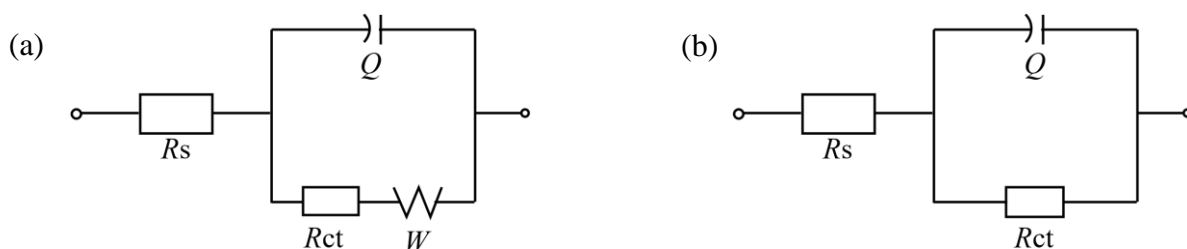


Figure 3. Equivalent circuit models for lime soil at different curing times: (a) 1 d, 2 d and 3 d, (b) 7 d, 14 d, 21 d and 28 d.

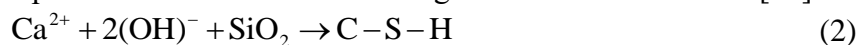
The lime soil is a cementitious material. Many available studies[4, 20-23] show that the typical reactions in lime soil proceed through these four basic mechanisms:

(1) Ion exchange: $\text{Ca}(\text{OH})_2$ in hydrated lime is a strong electrolyte. When hydrated lime is mixed with the soil, the Ca^{2+} ions from $\text{Ca}(\text{OH})_2$ exchange with Na^+ , K^+ , and H^+ ions in the soil. The ions adsorbed on the surfaces of the soil particles change from monovalent to divalent, which reduces the thickness of the adsorbed water film on the surface of the soil particles, and the soil particles are closer together as a result. Thus, the mineral particles aggregate and the thickness of the diffuse double layer decreases. Ion exchange reactions take place during the first 3 d of curing[24].

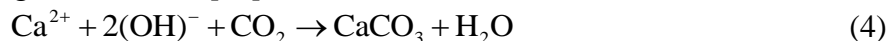
(2) Flocculation and agglomeration: the reaction of $\text{Ca}(\text{OH})_2$ with water results in a crystalline polymer, and its chemical reaction equation is:



(3) Pozzolanic reactions: silica and alumina, which dissolve from clay minerals, combine with Ca^{2+} to form calcium silicate hydrates (C-S-H) and calcium aluminate hydrates (C-A-H). These C-S-H and C-A-H products fill the soil matrix and increase the shear strength and unconfined compressive strength of lime soil. Moreover, the pozzolanic reactions have a long-term effect on lime soil[21].



(4) Carbonation: Carbonation refers to the reaction between $\text{Ca}(\text{OH})_2$ and atmospheric CO_2 , and it has a minor effect on the strength of lime soil[20].



The results of electrochemical impedance spectroscopy measurements, Nyquist plots of lime soil at different curing times, are shown in

Figure 2. According to the topological structure of the Nyquist plots and the reaction mechanism of lime soil, the EIS results can be divided into two stages for discussion and analysis: the initial stage (1 d, 2 d and 3 d) and the relatively stable stage (7 d, 14 d, 21 d and 28 d). In the initial stage, the Nyquist plots combine a semicircle and a 45° straight line. In the relatively stable stage, the Nyquist plots contain a series of semicircles with different radii at different curing times. As the curing time increases, the radii of the semicircles increase in both stages.

With reference to the equivalent circuit model of the hydration process of cement and concrete, the equivalent circuit model for the two stages shown in Figure 3 can be described as $R_s(Q(RctW))$ and $R_s(QRct)$ according to the circuit description code (CDC)[25-27]. The former model is often known as the Randles equivalent circuit model where R_s is the resistance of the electrolyte solution; Q is the double layer capacitance related to the diffuse double layer; Rct corresponds to the resistance of the charge transfer procedure in the pozzolanic reaction; and W stands for the Warburg resistance caused by charge diffusion during ion exchange.

Thus, Q and Rct have strong connections to the strength of lime soil. It is important to note that the latter equivalent circuit model has one fewer circuit elements (Warburg resistance) than the former. This is because ion exchange usually occurs in the initial stage[24, 28].

The EIS results were analysed with ZSimpWin3.60 software. The fitting lines are shown in Figure 2, and the calculated equivalent circuit element parameters are listed in

Table 3. They indicate that the two models are both suitable for fitting the electrochemical impedance spectroscopy spectra, and the chi-square (χ^2) value is minimized to 10^{-4} .

Table 3. Calculated equivalent circuit element parameters.

Stage	Age (d)	R_s ($\Omega \cdot \text{cm}^2$)	R_{ct} ($\text{k}\Omega \cdot \text{cm}^2$)	Q ($\mu\text{F}/\text{cm}^2$)	W ($\text{S} \cdot \text{s}^{-0.5}/\text{cm}^2$)
Initial stage	1	1077	3.21	25.39	789.1
	2	1157	6.88	22.77	2271.6
	3	1219	13.18	19.47	3490.5
Relatively stable stage	7	1337	368.15	18.31	—
	14	1492	531.65	16.79	—
	21	1921	774.33	8.64	—
	28	2010	932.07	7.83	—

3.2.2. Bode plots

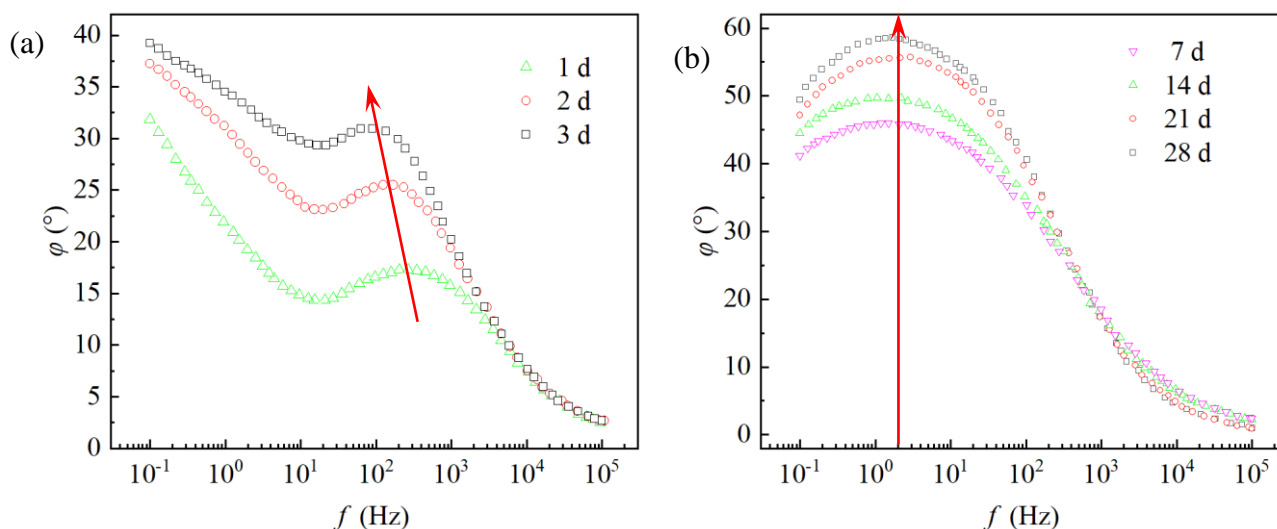


Figure 4. Bode plots for lime soil at different curing times: (a) 1 d, 2 d and 3 d, (b) 7 d, 14 d, 21 d and 28d.

Table 4. The peak phase angle values ($\varphi_{P_{max}}$) at different curing times.

Stage	Initial stage			Relatively stable stage			
Age/(d)	1	2	3	7	14	21	28
$\varphi_{P_{max}} / (^\circ)$	17.49	25.72	31.15	45.98	50.10	55.90	58.66

Based on the Bode plots in Figure 4(a) and (b), there is only one peak on the φ - f curve at each curing time. In the initial stage, the peak moves in the low-frequency direction. In the relatively stable stage, the peak appears at a frequency of approximately 1.5 Hz. The peak appears at low frequency, and its value increases as the curing time increases, which indicates that the peak phase angle at low frequency may be used to assess the compactness of lime soil. When the peak phase angle is larger, the lime soil is more compact[29]. The peak phase angle values ($\varphi_{P_{\max}}$) at different curing times are listed in Table 4.

3.3. Relationships between EIS results and shear strength

3.3.1. Shear strength

Shear strength parameters include the internal friction angle (φ) and cohesion (c), which are usually determined by Mohr-Coulomb failure criteria. The internal friction angle and cohesion of lime soil measured by the triaxial compressive test are summarized in Table 5. These results show that both the internal friction angle and cohesion increase with curing time. However, the increase in the angle of internal friction is small. On the other hand, the cohesion has a slight, insignificant increase during the initial stage and a significant increase during the relatively stable stage. This is due to the long-term pozzolanic reactions, which generate more C-S-H and C-A-H as the curing time increases.

Table 5. Internal friction angle and cohesion of lime soil at different curing times.

Stage	Age/(d)	Internal friction angle(φ)/(°)	Cohesion (c)/(kPa)
Initial stage	1	27.78	60.46
	2	27.83	67.52
	3	27.86	75.68
Relatively stable stage	7	27.94	96.53
	14	28.14	120.67
	21	28.56	142.66
	28	28.77	163.59

3.3.2. Relationship between the internal friction angle (φ) and the peak phase angle value ($\varphi_{P_{\max}}$)

As noted in the preceding text, when the peak phase angle is larger, the lime soil is more compact. We thus consider using the peak phase angle value ($\varphi_{P_{\max}}$) to assess the internal friction angle (φ). Their relationship is shown in Figure 5. There are linear relationships for these two stages, and there is a

significant inflection point at 7 d. R^2 values, which are close to 1, indicate good fits.

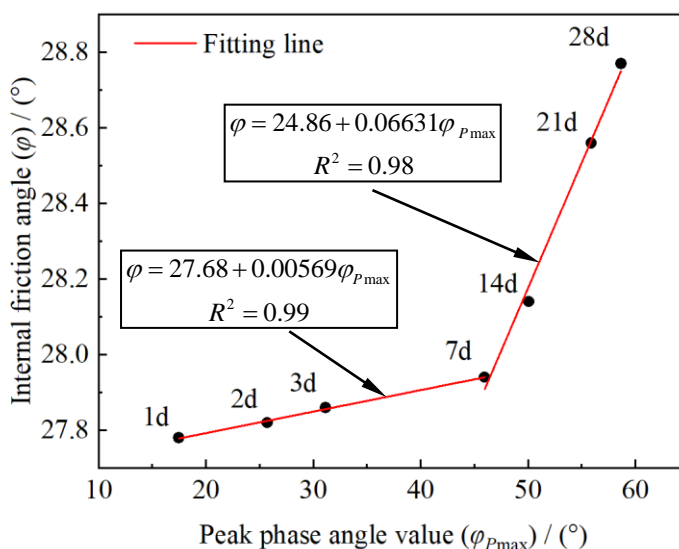


Figure 5. Relationship between the internal friction angle (φ) and the peak phase angle value ($\varphi_{P_{max}}$).

3.3.3. Relationship between cohesion and Rct/Q

Cohesion is closely related to the curing time and pozzolanic reactions[30]. The equivalent circuit element parameters Rct and Q can characterize the pozzolanic reactions at different curing times. Cohesion is positively correlated with Rct and negatively correlated with Q . Thus, cohesion can be characterized by Rct/Q (the ratio of Rct and Q). The relationship between cohesion and Rct/Q is shown in Figure 6. It can be seen from Figure 6 that there are strong linear relationships between the cohesion and $\ln(Rct/Q)$. There is a significant inflection point at 7 d.

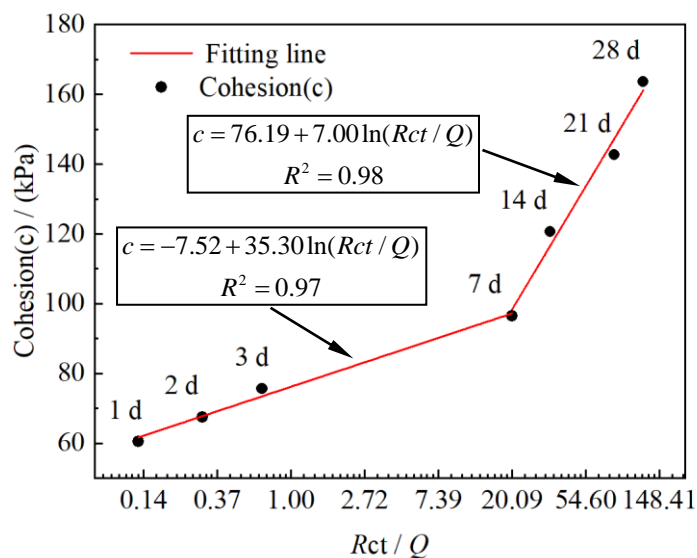


Figure 6. Relationship between cohesion and Rct/Q

3.4. Relationships between EIS results and the unconfined compressive strength (q_u)

3.4.1. Unconfined compressive strength (q_u)

The unconfined compressive strength of lime soil at different curing times is listed in

Table 6 and shows the effect of curing time on the unconfined compressive strength. The unconfined compressive strength increases with increasing curing time. However, the unconfined compressive strength increases less rapidly in the initial stage, which can be explained by exchanges with Ca^{2+} , Na^+ , K^+ , and H^+ . The unconfined compressive strength increases significantly in the relatively stable stage because the pozzolanic reaction is the primary reaction during this stage.

Table 6. Unconfined compressive strength at different curing times.

Stage	Initial stage				Relatively stable stage			
Age/(d)	1	2	3	7	14	21	28	
q_u /(kPa)	618	646	680	764	945	1260	1410	

3.4.2. Relationship between q_u and Rct/Q

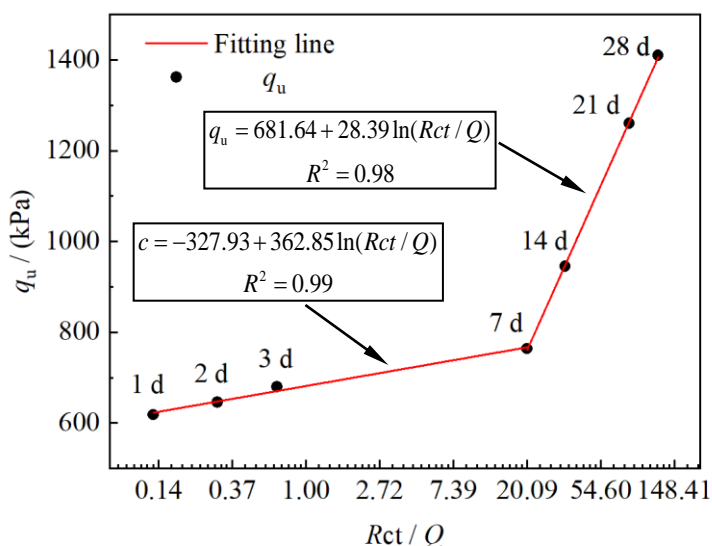


Figure 7. Relationship between q_u and Rct/Q

Zhu et al. [3] considered that the increase in the unconfined compressive strength of lime soil is due to aggregated soil particles, which are significantly associated with C-S-H and C-A-H. In addition, it is obvious that the correlation between the unconfined compressive strength and Rct shows a positive tendency, and the correlation between the unconfined compressive strength and Q shows a negative

tendency.

Thus, the unconfined compressive strength can be characterized by Rct/Q (the ratio of Rct and Q). The relationship between the unconfined compressive strength and $\ln(Rct/Q)$ is shown in Figure 7. There is a significant inflection point at 7 d. The linear relationships ($R^2 \geq 0.98$) indicate excellent agreement between the unconfined compressive strength and $\ln(Rct/Q)$.

4. CONCLUSIONS

Lime soil samples (3:7) with curing times of 1 d, 2 d, 3 d, 7 d, 14 d, 21 d and 28 d were tested by electrochemical impedance spectroscopy (EIS), triaxial compressive tests and unconfined compression tests. The following conclusions can be drawn:

(1) The EIS results for 3:7 lime soil can be divided into two stages: the initial stage (1 d, 2 d and 3 d) and the relatively stable stage (7 d, 14 d, 21 d and 28 d). In the initial stage, the Nyquist plots correspond to the classic Randles model; in the relatively stable stage, the Nyquist plots contain a series of semicircles with different radii. In both stages, there is only one peak in the Bode plots, and the peak phase angle value ($\varphi_{p_{max}}$) increases with increasing curing time. The two-stage EIS results can well reflect the chemical reactions in lime soil for different curing times. The impedance change measured by EIS can be applied to assess the shear strength and unconfined compressive strength of lime soil.

(2) The R_s ($Q(RctW)$) and R_s ($QRct$) equivalent circuit models can accurately fit the measured EIS data, where the agreement between the EIS spectra and the equivalent circuit models is excellent. The equivalent circuit element parameters are closely related to the typical reactions in lime soil, which have a significant effect on shear strength and unconfined compressive strength.

(3) The peak phase angle value ($\varphi_{p_{max}}$) can be used to assess the internal friction angle (φ). In these two stages, there is good linearity between the internal friction angle (φ) and the peak phase angle value ($\varphi_{p_{max}}$), and the correlation coefficient values (R^2) are greater than 0.98.

(4) The equivalent circuit element parameters Rct and Q can characterize the pozzolanic reactions at different curing times; therefore, they can be used to assess the cohesion (c) and unconfined compressive strength (q_u). Rct is positively associated with c and q_u , while Q is negatively associated with these parameters. The goodness of fit demonstrated good linear relationships between cohesion and $\ln(Rct/Q)$ and between unconfined compressive strength and $\ln(Rct/Q)$.

(5) Clear linear correlations were established between the EIS parameters and strength of lime soil, which directly supports the feasibility of using EIS results to evaluate the shear strength and unconfined compressive strength of lime soil for different curing times. This study offers a promising approach to evaluate the strength of lime soil by EIS testing.

ACKNOWLEDGEMENTS

The present work is supported by the National Natural Science Foundation of China (No: 41807256).

References

1. W. Alex, H. Asadul, K. Jayantha, A. John and C. David, *J. Geotech. Geoenviron.*, 136 (2010) 1459.
2. K. Arvind, S. W. Baljit and B. Asheet, *J. Mater. Civil Eng.*, 19 (2007) 242.
3. F. Zhu, Z. C. Li, W. Z. Dong and Y. Y. Ou, *B. Eng. Geol. Environ.*, 78 (2019) 2345.
4. A. K. Jha and P. V. Sivapullaiah, *Indian Geotechnical Journal*, 50 (2020) 339.
5. L. Jacques, B. Marc-André and C. Marc, *NRC Research Press Ottawa, Canada*, 27 (1990) 294.
6. I. B. D., G. S. and D. F. R. C., *Géotechnique*, 51 (2001) 533.
7. P. Elena, D. Dimitri, G. Anne-Claire, P. Michael and O. Guy, *Cement Concrete Res.*, 42 (2012) 626.
8. A. B. Jair, B. M. Ecclesielter, T. Wagner, L. S. I. Ronaldo and L. R. Juliana, *J. Rock Mech. Geotech. Eng.*, 10 (2018) 188.
9. B. Q. Dong, G. Li, J. C. Zhang, Y. Q. Liu, F. Xing and S. X. Hong, *Constr. Build. Mater.*, 149 (2017) 467.
10. C. M., M. P., M. A., R. N. X. and S. I., *Cement Concrete Res.*, 32 (2002) 881.
11. B. Q. Dong, J. H. Zhang, Y. Q. Liu, G. H. Fang, Z. Ding and F. Xing, *Constr. Build. Mater.*, 113 (2016) 997.
12. J. Ren, J. H. Zhang, X. F. Wang, D. F. Li, N. X. Han and F. Xing, *Cem. Concr. Compos.*, 114 (2020) 103776.
13. L. Chi, Z. Wang, S. Lu, D. Z. Zhao and Y. Yao, *Constr. Build. Mater.*, 208 (2019) 659.
14. D. J. A. B. Jair, L. D. S. I. Ronaldo, B. M. Ecclesielter and L. R. Juliana, *J. Rock Mech. Geotech. Eng.*, 11 (2019) 882.
15. D. Deneele, A. Dony, J. Colin, G. Herrier and D. Lesueur, *Mater. Struct.*, 54 (2021) 1359.
16. K. Bairlein, A. Hördt and S. Nordsiek, *Near Surf. Geophys.*, 12 (2014) 667.
17. H. N. A. Gowda Ramesh and P. V. B. Sivapullaiah, *P. I. CIVIL. ENG-MAR. EN.*, 164 (2010) 15.
18. X. Sun, M. J. Zhao, K. Wang and JZ. Lin, *Sens. Transducers*, 159 (2013) 431.
19. M. A. M. D. Di Sante, *Geotech. Geol. Eng.*, 38 (2020) 2335.
20. S. Diamond and E. Kinter, *Highway Research Record*, 92 (1965) 83.
21. F. G. Bell, *Eng. Geol.*, 42 (1996) 223.
22. N. C. Consoli, L. D. S. Lopes, P. D. M. Prietto, L. Festugato and R. C. Cruz, *J. Geotech. Geoenviron.*, 137 (2011) 628.
23. P. Akula and D. N. Little, *MethodsX*, 7 (2020) 100928.
24. M. Di Sante, E. Fratolocchi, F. Mazzieri and E. Pasqualini, *Appl. Clay Sci.*, 99 (2014) 100.
25. M. L. Shi, Z. Y. Chen and J. Sun, *Cem. Concr. Res.*, 29 (1999) 1111.
26. B. Q. Dong, Q. W. Qiu, J. Q. Xiang, C. J. Huang, F. Xing and N. X. Han, *Materials*, 7 (2014) 218.
27. B. Q. Dong, Q. W. Qiu, Z. T. Gu, J. Q. Xiang, C. J. Huang, Y. Fang, F. Xing and W. Liu, *Cem. Concr. Compos.*, 65 (2016) 118.
28. J. H. Smith, *Lime Stabilization*, Thomas Telford Limited, (1996) London, United Kingdom.
29. G. L. Tao, C. C. Gao and Z. Y. Qiao, *Int. J. Electrochem. Sc.*, 12 (2017) 11692.
30. M. R. A. C. Aemail, A. Ghalandarzadeh and L. S. Chafi, *J. Rock Mech. Geotech. Eng.*, (2021) in press.